European Journal of Radiology Open 3 (2016) 172–181

Contents lists available at ScienceDirect

European Journal of Radiology Open

journal homepage: www.elsevier.com/locate/ejro

From first to latest imaging technology: Revisiting the first mummy investigated with X-ray in 1896 by using dual-source computed tomography

Stephanie Zesch[a,*], Stephanie Panzer[b,c], Wilfried Rosendahl[a], John W. Nance Jr.[d], Stefan O. Schönberg[e], Thomas Henzler[e]

[a] Reiss-Engelhorn-Museen, Museum Weltkulturen D5, 68159 Mannheim, Germany
[b] Department of Radiology, Trauma Center Murnau, Prof.-Kuentscher-Strasse 8, 82418 Murnau, Germany
[c] Institute of Biomechanics, Trauma Center Murnau and Paracelsus Medical University Salzburg, Prof.-Kuentscher-Strasse 8, 82418 Murnau, Germany
[d] Department of Radiology, Massachusetts General Hospital, Harvard University, Boston, MA, USA
[e] Institute of Clinical Radiology and Nuclear Medicine, University Medical Center Mannheim, Medical Faculty Mannheim—Heidelberg University, Theodor-Kutzer-Ufer 1-3, 68167 Mannheim, Germany

ARTICLE INFO

Article history:
Received 30 June 2016
Accepted 2 July 2016
Available online 25 July 2016

Keywords:
X-ray
Dual-energy computed tomography
Child mummy
Ancient Egypt
Pectus excavatum deformity
Hepatomegaly

ABSTRACT

Purpose: The aim of this study was to systematically reinvestigate the first human mummy that was ever analyzed with X-ray imaging in 1896, using dual-source computed tomography (DSCT) in order to compare the earliest and latest imaging technologies, to estimate preservation, age at death, sex, anatomical variants, paleopathological findings, mummification, embalming and wrapping of the child mummy from ancient Egypt. Radiocarbon dating was used to determine the mummy's age and to specify the child's living period in the Egyptian chronology.
Material and methods: The ancient Egyptian child mummy is kept in the *Senckenberg Museum of Natural History* in Frankfurt am Main, Germany. An accelerator mass spectrometer (MICADAS) was used for radiocarbon dating. DSCT was performed using a 2 × 64 slice dual-source CT system (Siemens Healthineers, Forchheim, Germany). A thorough visual examination of the mummy, a systematic radiological evaluation of the DICOM datasets, and established methods in physical anthropology were applied to assess the bio-anthropological data and the post mortem treatment of the body.
Results: Radiocarbon dating yielded a calibrated age between 378 and 235 cal BC (95.4% confidence interval), corresponding with the beginning of the Ptolemaic period. The mummy was a male who was four to five years old at the time of death. Remnants of the brain and inner organs were preserved by the embalmers, which is regularly observed in ancient Egyptian child mummies. Skin tissue, inner organs, tendons and/or musculature, cartilage, nerves and vasculature could be identified on the DSCT dataset. The dental health of the child was excellent. Anatomical variants and pathological defects included a congenital *Pectus excavatum* deformity, hepatomegaly, Harris lines, and longitudinal clefts in the ventral cortices of both femora.
Conclusion: Our results highlight the enormous progress achieved form earliest to latest imaging technology for advanced mummy research using the first human mummy investigated with X-ray. With the application of DSCT, detailed knowledge regarding age at death, sex, diseases, death, and mummification of a child from Ptolemaic Egypt are revealed while considering the temporary rites of body treatment and burial for children.
© 2016 The Authors. Published by Elsevier Ltd. This is an open access article under the CC BY-NC-ND license (http://creativecommons.org/licenses/by-nc-nd/4.0/).

1. Introduction

A few months after the discovery of X-rays by Wilhelm Conrad Roentgen in November 1895, the physicist Walter Koenig conducted the first radiographic investigation of mummified remains at the *Physical Society of Frankfurt a.M.*, Germany. The results of this investigation were published in March 1896 in the monograph

* Corresponding author.
E-mail address: stephanie.zesch@mannheim.de (S. Zesch).

http://dx.doi.org/10.1016/j.ejro.2016.07.002
2352-0477/© 2016 The Authors. Published by Elsevier Ltd. This is an open access article under the CC BY-NC-ND license (http://creativecommons.org/licenses/by-nc-nd/4.0/).

entitled *14 Photographs with X-rays taken by the Physical Society of Frankfurt am Main* [1]. The X-rayed objects included a bandaged ancient Egyptian child mummy from the *Senckenberg Museum of Natural History* (inventory number ÄS 18).

The earliest radiographic investigations of mummies focused on discovering amulets and jewelry within the body cavities, evaluating the wrappings, and determining whether human or animal bones were represented in bandages and coffins [2,3]. However, the application of the novel X-ray technique included shortly afterwards the aim of assessing anthropological and paleopathological knowledge about the mummified individuals [2,4–6].

The abilities of paleoradiology were greatly enhanced with the introduction of computed tomography (CT) in the early 1970s, allowing non-invasive analysis of body cavities (e.g. cross-section) for the first time [7]. Peter Lewin and Derek Harwood-Nash performed the first axial CT examination of mummified tissue from ancient Egypt at the Hospital of Sick Children in Toronto in 1976 [7,8]. They investigated the desiccated brain of Nakht, a 21st dynasty mummy of an adolescent male in the collection of the Royal Ontario Museum in Toronto; this was followed by the first complete body scan on the female mummy of Djedmaatesankh, from the 22nd dynasty, housed within the same museum [9].

CT imaging is now widely used in mummy research in order to non-invasively assess a variety of parameters, including bone and soft tissue preservation, post-mortem damages, artifacts, mummification technique, embalming, age at death, sex, diseases, trauma, cause of death, medical intervention, and artificial cranial deformation [5,10].

In this case study, the ancient Egyptian child mummy from *Senckenberg Museum of Natural History*, which was the first mummy ever investigated with X-rays, was reanalyzed in an interdisciplinary approach using dual-source computed tomography (DSCT), radiocarbon dating, and physical anthropology.

2. Material and methods

2.1. Provenance and outer appearance

In 1817, the natural scientist and Africa explorer Eduard Rueppell collected numerous objects from ancient Egypt on his first trip to Africa, including small size Aegyptiaca, mummies and sarcophagi. Purchasing these objects was possible due to personal funding of the explorer and with the support of ingenious collectors. At first, the objects were transferred to the *Senckenberg Museum of Natural History* in Frankfurt am Main, Germany, then afterwards to the *Historical Museum Frankfurt*. Later, the *Historical Museum Frankfurt* left the Aegytiaca to the *Liebieghaus* and returned the mummies, sarcophagi and some animal trophies to the *Senckenberg Museum of Natural History* in 1970. The child mummy (Fig. 1) is about 80 cm in length, with a maximum width of 24 cm on shoulders and maximum depth of 16 cm on the head. There is no iconographical or textual decoration to facilitate identification or chronological dating of the mummy. Both arms are aligned laterally to the body, while the left hand is displaced slightly anteriorly on the left thigh. The head, arms, fingers and legs are individually wrapped with textile (probably linen) in tightly packed layers. The body, however, is incompletely covered, likely due to post-preservation removal of some wrapping material. The cranial vault is largely free of textile tissue and the preserved layers are much thinner than those of the body. Wrapping material is also absent on the back of the left hand, the left thumb, the left second phalanx and on all phalanges of the right hand. The left thigh, left lower leg, and right lower leg are partially free of soft tissue and wrappings. All tissue damage was probably caused postmortem. The textile wrappings are soaked with dark bitumen based embalming liquids, especially on the head and extremities.

Fig 1. Photography of the bandaged ancient Egyptian child mummy from the *Senckenberg Museum of Natural History* in Frankfurt a.M. (inventory number ÄS 18).

2.2. Radiocarbon dating

For estimating the post mortem interval (PMI) of the mummy, approximately 1 g of soft tissue was sampled in a minimal invasive way by using a previously existing hole in the textile wrap-

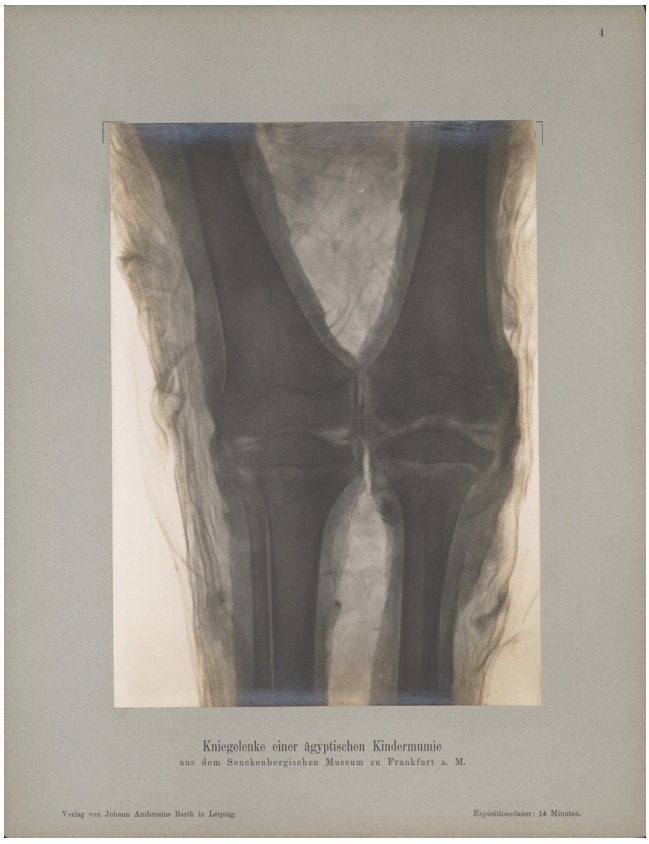

Fig. 2. Reproduction of the historical X-ray image of the child mummy's knees (© German Röntgen Museum, Remscheid-Lennep, Germany). The image shows the mirror-inverted perspective of the knees, which happened when the negative image was transferred into positive.

ping of the left thigh. To mitigate possible contamination with embalming substances, the material was purified with organic solutions (benzene, acetone) and treated with the ABA method (Acid/Base/Acid, HCl/NaOH/HCl). Sample preparation and measurements were conducted by an accelerator mass spectrometer (AMS) of type MICADAS.

According to the international consensus, ^{14}C or AMS ^{14}C age are the conventional readings obtained by radiocarbon dating. The measured data is specified as a numerical value with a standard deviation (±value) and followed by the symbol BP (Before Present), meaning the reference year 1950 [11]. ^{14}C data are known to be systematically low by three percent, and the temporally variable data are not factored into the initial ^{14}C ratio; therefore, the dates have to be calibrated into calendar years. The calibrated ages are followed by the symbol cal BC (calibrated before Christ) as calendar age. Calibration of data was conducted using INTCAL13 and SwissCal 1.0 software.

Fig. 3. Thick mean intensity coronal multi-planar reconstruction of the lower extremities of the mummy. The image shows the body in the correct anatomical position.

2.3. First X-raying by Walter Koenig

In 1896, several objects – including the child mummy investigated in this study – underwent conventional radiography by Walter Koenig at the *Physical Society of Frankfurt am Main*, Germany. Koenig's descriptions of the X-ray technique are provided below, translated from the original German citation: *"[. . .] The applied experimental design differed from the one used in other places in a way that the vacuum tube for generating X-rays – let's call it X-ray lamp – was not stimulated by a simple inductor, but by a Tesla transformer powered by an inductor in the way Himstedt specified. The X-ray lamp was not a pear-shaped tube with a big, flat cathode as it was usually applied, but a globe-shaped tube with a concave mirror cathode and a central platinum plate, like it was produced by glassblowers, to show the warming effect of cathode radiation. Al shots are made with this tube manufactured by F. O. R. Goetze at Leipzig. The distance between the photographic plates and the center of the glass bulb was averagely about 25 centimeters. The plates were embedded in wooden caskets or in lightproof envelopes and the documented objects directly above those envelopes, to protect the plates from ambient light. All images were taken on Schleussner plates with a strong rodinal solution for development. The positive images, which are included inside this map, are created by using the latest rotation and kilometer method on Bromaryt Paper of the New Photographic Society Schöneberg-Berlin [. . .]"*

Table 1
Summary of CT scan parameters.

	Dual-Energy CT	Single Energy CT
Tube Voltage	140/80 kVp	120 kVp
Tube current	80/110 ref. mAs	300 ref. mAs
Pitch	0.55	1.4
Detector collimation	$2 \times 32 \times 0.6$	$2 \times 32 \times 0.6$
Slice thickness	0.6 mm	0.6
Reconstruction increment	0.3 mm	0.3 mm
Reconstruction kernel	D10f; D60f	B20f; B60f

[1]. The knee joints of the mummy were exposed to the X-ray tube for approximately 14 min [1].

2.4. Scanning the mummy with dual-source CT

In 2013, the mummy was re-examined using a 2×64 slice 1st generation DSCT system (SOMATOM Definition, Siemens Healthineers, Forchheim, Germany). The mummy was scanned twice, using both single energy and dual-energy techniques. Scan acquisition parameters and image reconstruction parameters are summarized in Table 1. Post processing of the DICOM files was performed by the medical imaging software OsiriX™ (3.7.1, 64-bit, Pixmeo SARL, Geneva, Switzerland). Image analysis was done using two-dimensional (2D) image analysis, multiplanar three-dimensional (3D) reconstruction, and volume rendering reconstructions (VRTs).

2.5. Applied methods for assessing preservation, age at death and sex

The checklist by Panzer et al. was applied to the whole-body CT for evaluation of the soft tissue preservation. This checklist is divided into assessing the soft tissues of the head and musculoskeletal system (main category A) and organs and organ systems (main category B) [12].

Determination of age at death was conducted by assessing tooth development and eruption [13], primary ossification centers of hand bones, fusion of epiphysis and skull sutures [14] and length of long hollow bones [15]. The most obvious indicator for sex determination in the case of mummified corpses, which is the presence of external genitalia, could not be assessed through the outer examination because of the mummy's wrapping. Morphological methods for sex estimation, as described for example by Schutkowski [16], may be suitable for skeletal remains of non-adults but are less useful for mummified corpses. In our case, sex determination was available via detailed soft tissue analysis of CT data.

3. Results

3.1. Radiocarbon dating

The soft tissue sample (laboratory number MAMS 22577) yielded a ^{14}C age of 2247 ± 23 years BP and a calibrated age between 378 and 235 years cal BC (95.4% confidence interval), meaning the child lived at the beginning of Ptolemaic period, which covered a time span from 332 BC to 30 BC [17].

3.2. First X-raying by Walter Koenig

Fig. 2 shows the historical X-ray image of the child mummy's knees made by Walter Koenig in 1896 (Fig. 2). General observations deducted from the conventional X-ray images of several objects made by Koenig are provided in the following, translated from the original German citation: *"[. . .] for an adequate evaluation of the images, you have to consider that those objects or parts of objects which were placed more distantly from the plate and closer to the X-ray source, seem to be proportionally enlarged on the image; moreover, the sides of an object interchange when transferring the negative image into the positive. The images seem to show the upper side of an object as it was placed on the plate, however it's not the object itself but a mirror-inverted perspective [. . .]"* [1]. "[. . .] *the last shot* (means Fig. 2) *is a remarkable example for perspective distortions occasionally coming up with this kind of image; the plate didn't lie completely parallel to the legs of the mummy, the femora stood more distantly from the plate appearing to diverge in an abnormal way on the image [. . .]"* [1].

Table 2
CT derived diameters of the preserved inner organs.

Inner organs	Laterolateral (mm)	Craniocaudal (mm)	Anteroposterior (mm)
Liver (complete)	70	100	45
Liver (right lobe)	80	100	45
Liver (left lobe)	22	25	21
Heart	30	40	20
Spleen	5	48	–
Kidney (right)	14	41	–
Kidney (left)	–	–	–

In order to compare the historical X-ray image with current CT imaging, a CT reconstruction of the mummy is presented (Fig. 3); it shows the correct anatomical position of the body, in contrast to the mirror-inverted perspective of the knees in the historical X-ray of 1896 (Fig. 2).

3.3. Re-examination of the mummy using dual-source/dual-energy CT

3.3.1. Bone and soft tissue preservation

Bone and soft tissue preservation of the bandaged mummy is quite good, and the skeleton is complete (Fig. 4). Several articular dislocations, which were probably caused post mortem, have been identified, for example both distal femora are anteriorly displaced relative to the knee joints. Redundant ventral skin tissue which is radiographically represented as several longitudinal discontinuities was identified along the anterior abdominal wall. This likely indicates a vaulting of the skin at time of death, possibly due to an abundant diet or a pathological condition.

Following the checklist described by Panzer et al. [12] resulted in a composite score of 145.5, including 92 for the head and musculoskeletal system (main category A) and 53.5 for organs and organ systems (main category B). These head checkpoints were detectable: nose, auricles, ossicles, bulb and/or lens, optic nerve, eye muscles and tentorium. All 16 proposed tendon/musculature checkpoints could be identified. From peri- and intra-articular soft tissues, the checkpoints rotator cuff, long biceps tendon, capsule and/or labrum were detectable for the shoulders. The capsule and/or labrum were present in both hips. Both knees revealed preservation of the medial and lateral meniscus. Intervertebral discs were present in the thoracic and lumbar spine. The entire body showed extraordinary preservation of cartilage tissue, which was particularly visible at the articulated joints of hands, sternum, pelvis, knees and feet. Concerning the central nervous system and peripheral nerves, the checkpoints for brain mass/fragments, spinal cord and/or dura for the cervical and thoracic spins and peripheral nerves for the cervical, thoracic, lumbar and sacral spine were present. Remnants of the brain are visible as a shrunken mass on the posterior cranial fossa and within the cervical spinal canal (Fig. 5). Differentiation between cerebrum and cerebellum was not possible. The dura mater, including the falx and tentorium, were attached to the more anterior parts of the skull. CT-derived diameters of the preserved inner organs are listed in Table 2. Remnants

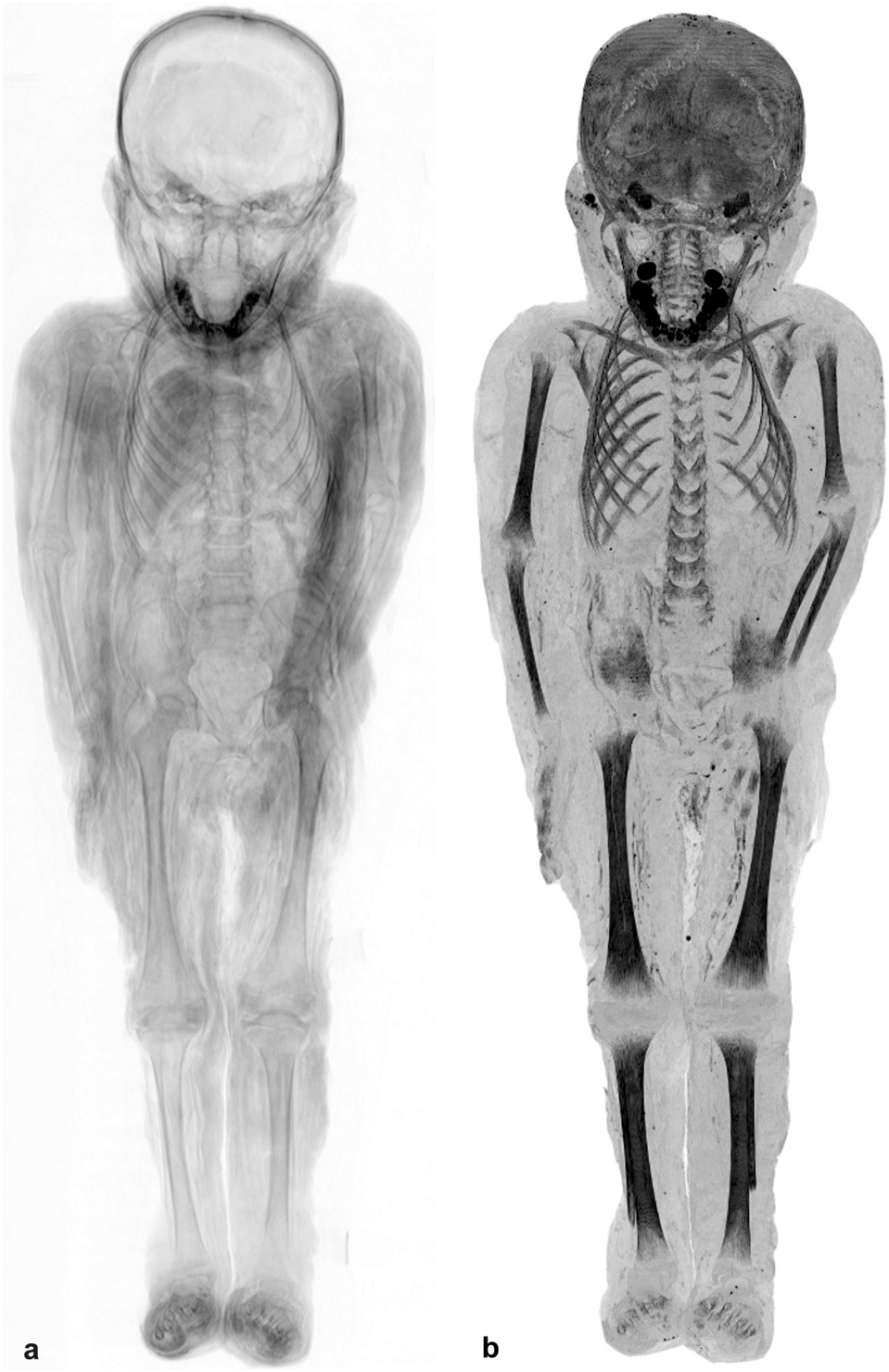

Fig. 4. Coronal whole body multi-planar reconstruction. The densely wrapped bandages are well preserved (a) and the skeleton of the mummy is completely preserved (b). Image (a) represents a coronal thick mean intensity projection whereas image (b) represents a thick maximum intensity projection.

of the lungs and diaphragm were preserved bilaterally inside the dorsal upper part of the thorax. The liver was the best-preserved inner organ on CT and had partially migrated into the thoracic cavity (Fig. 6). The heart was displaced into the upper part of the chest, likely due to migration of the liver into the chest cavity (Fig. 6). Individual heart chambers were not identifiable due to shrinkage of the organ, but remnants of the thymus are visible medially to the heart. Concerning the gastrointestinal system, the checkpoints tongue, intestine, rectum and/or anus, liver and spleen were detectable. The narrow, u-shaped spleen was identified at its expected anatomical position inside the upper left quadrant of the abdomen. An intra-abdominal mass containing the small and large intestines, and the left kidney is visible inside the lower left thorax and abdominal cavity. The kidneys, penis and scrotum could be identified. The right kidney with clearly identifiable parenchyma and renal pelvis is preserved adjacent to the right liver lobe. The intracranial carotid and pelvic arteries were detectable on vascular assessment.

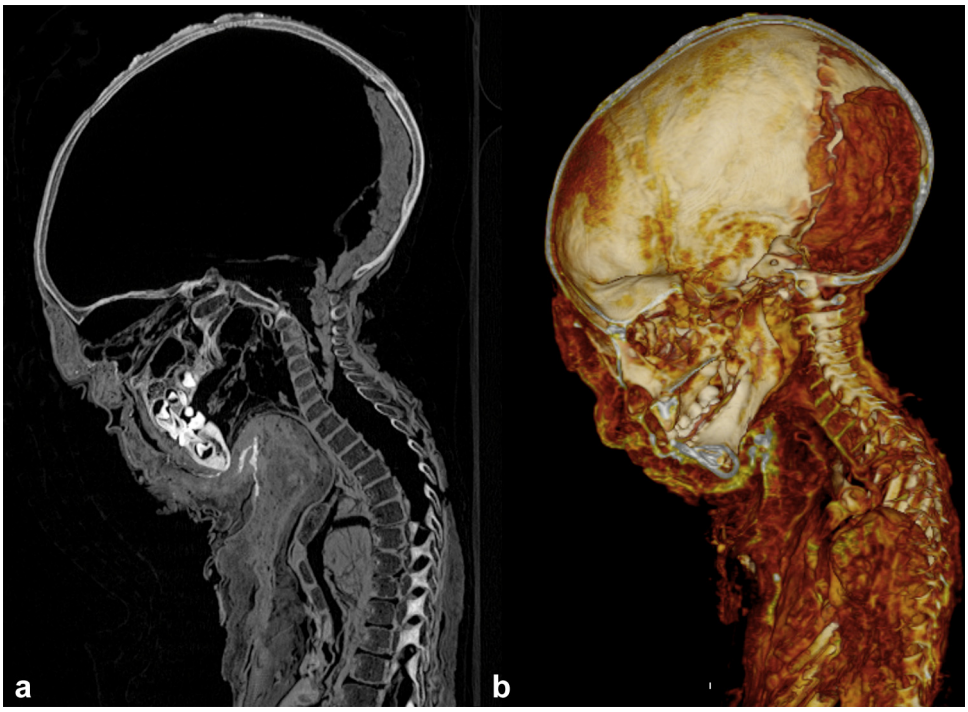

Fig. 5. Sagittal multi-planar reformation (a) and sagittal volume rendering reconstruction with plane clipping (b) demonstrates shrunken brain remnants of the child mummy within the posterior cranial fossa and within the cervical spinal canal. Image (a) also demonstrates the *Pectus excavatum* deformity.

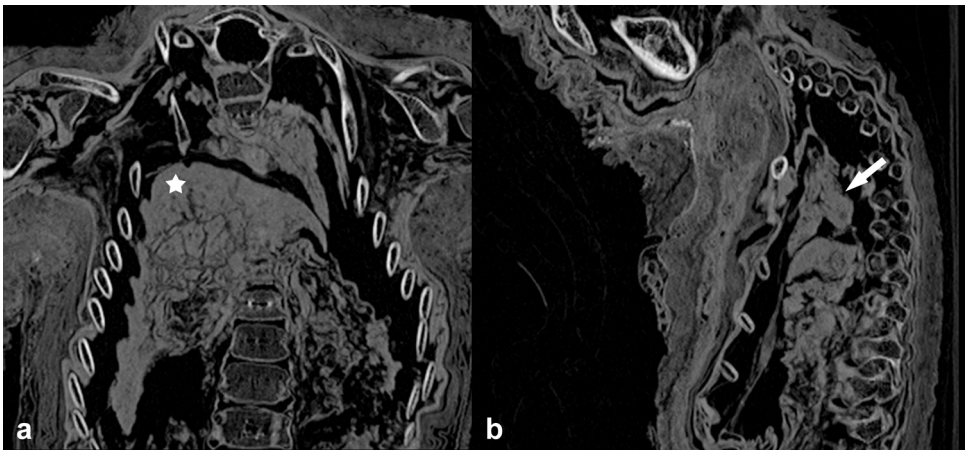

Fig. 6. Identified inner organs within the abdominal and thoracic cavity of the mummy. The white asterisk shows the well-preserved liver (a); the white arrow indicates the shrunken heart (b).

3.3.2. Age at death and sex

Dental and skeletal markers were assessed for age estimation. The mummy's deciduous teeth are entirely mineralized and erupted, but the permanent molar M1 had not yet erupted (Fig. 7), which indicates an age from four to five years [13]. The fused metopic suture and unfused posterior intra-occipital synchondrosis suggest an age between two and four years. Posterior fusion of the atlas, which usually occurs at an age of four to five years, was not ascertained. The degree of ossification and growth of the carpal bones, metacarpal bones and phalanges suggest a two-year-old child [14]. Long bone lengths suggest an age from two to three years [15]. The dental development which correlates more closely with chronological age than most of the other skeletal parts, seems to be under tighter genetic control [18], and is considered the most important marker for aging until early adolescence [19]. The mummy was therefore deemed to be four to five years old based predominantly on dentition.

Analysis of the CT data allowed visualization of the desiccated penis (Fig. 8), scrotum, and inguinal canal, identifying the mummy as male.

3.3.3. Anomalies, anatomical variants and paleopathological findings

3.3.3.1. Skull and dentition. Dentition was excellent, with no dental pathology. No cranial or cervical trauma was detected that could have had caused the child's death.

3.3.3.2. Thorax and abdominal cavity. Thoracic analysis revealed a soft tissue depression with a s-form configuration of the sternum demonstrating a maximum depth of about 8 mm at xiphosternal junction (Fig. 9), and a slightly oblique deposition of the sternum. Moreover, the xiphoid process shows a dorsal-inferiorly oriented

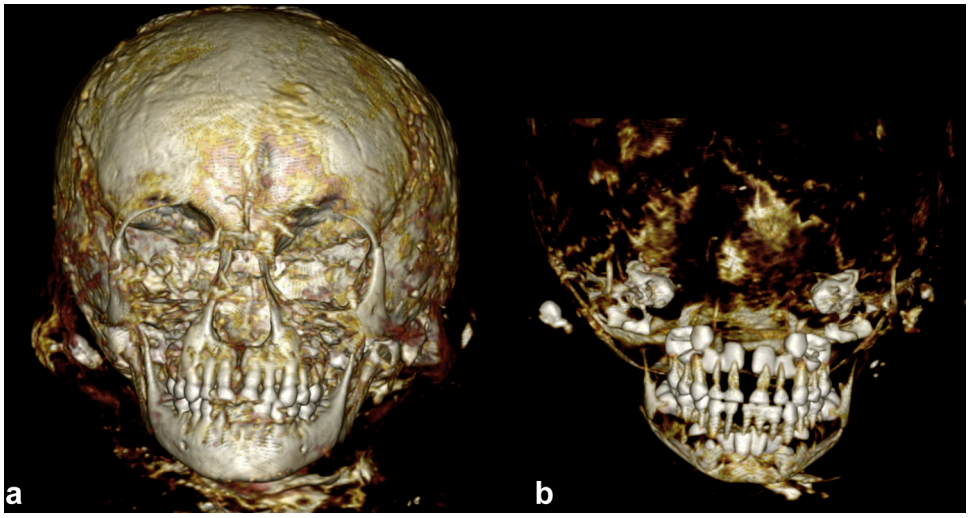

Fig. 7. Volume rendering reconstructions of the mummy's dentition status. Tooth development and eruption of the child in overview (a) and detail (b) indicate an age at death from four to five years.

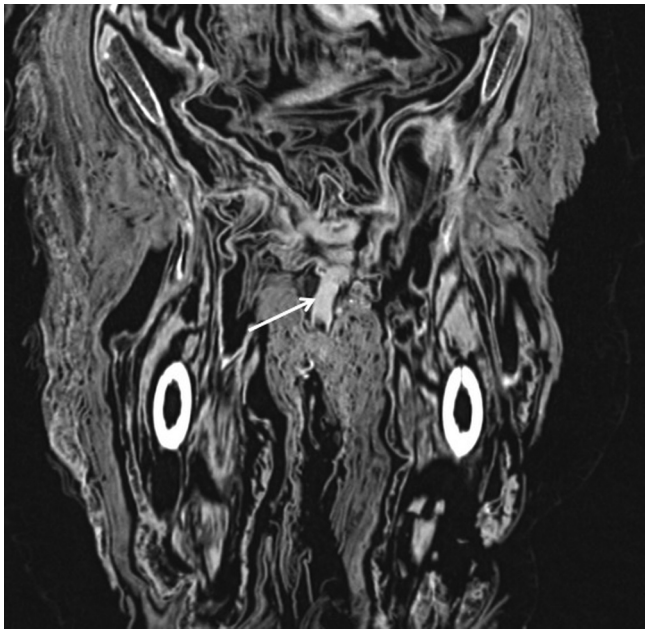

Fig. 8. Multi-planar 2D-reconstruction of the desiccated penis (white arrow).

kink. The area is largely covered with cutis. Bony and cartilaginous lesions suggesting a post mortem etiology of this abnormality are not visible; we therefore believe the child had *Pectus excavatum* morphology, as described in literature, for example by Koumbourlis [20].

The liver appears to be abnormally enlarged (Fig. 6, Table 2) compared to indexed values [21] and was probably even larger during life, indicating hepatomegaly. It is unclear whether there is associated splenomegaly.

3.3.3.3. Vertebral column and pelvis. Several anatomical variants of the spine are visible, including bilateral C7 cervical ribs (up to 1.2 cm on the right), a small rib/hyperplastic transverse process originating from L1 on the left, and a left L5-S1 segmentation defect.

There was mild thoracolumbar (dextro- or levo-) curvature [<10] or scoliosis [>10]; it is unclear whether this was positional or pathologic. A broad protrusion of the L4-L5 and L5-S1 intervertebral discs was detected.

Fig. 9. Sagittal multi-planar reconstruction of the thorax. The white arrow indicates a soft tissue depression of the thorax and a s-form configuration of the sternum, which is identified as a congenital *Pectus excavatum* deformity.

A subchondral lesion (5×5 mm) is visible in the right iliac bone adjacent to the sacroiliac joint representing a subchondral cyst or an intraosseous ganglion.

3.3.3.4. Extremities. The so called Harris lines which are visible as transverse lines of increased radio-opacity were detected on distal femoral metaphysis, proximal and distal tibia metaphysis, and distal fibular metaphysis.

Both femora showed a longitudinal cleft of the ventral cortex running parallel from the level of the lesser trochanter to the distal femoral metaphysis while leaving the femoral epiphyses intact (Fig. 10). Assessment of accompanying soft tissue damage was lim-

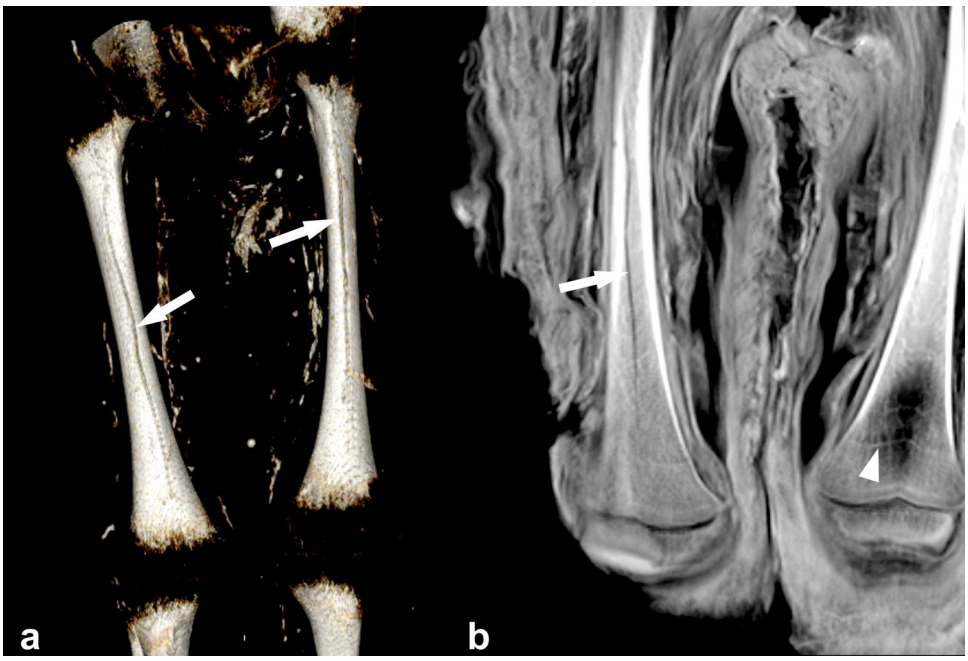

Fig. 10. 3D volume rendering (a) and multi-planar reconstruction (b) of a longitudinal cleft in the ventral cortical bone of both femora from the lesser trochanter to the distal metaphysis. Image (b) further shows Harris lines within the left distal femur (white triangle).

ited due to the intense shrinkage of the adjacent soft tissues and the folded skin of the thighs.

3.3.3.5. Mummification, embalming and wrapping. Remnants of the shrunken brain were visible inside the skull cavity. The body cavities were intact and the desiccated inner organs were present; several could be clearly identified (see 3.3.1.). Soft tissues are remarkably shrunken compared to the surrounding wrappings, particularly on the extremities.

Irregular foreign substances measuring up to 2079 HU were identified inside the auricles and near the opening of internal auditory canal on both sides.

Outer damage of wrappings was previously described (see 2.1.). The body shows a very thick modeling of bandages, especially on the mummy's face and the upper arms; the maximum axial bandage thickness was 1.6 cm on the right and 2.2 cm on the left upper arm. Hyperdense linear structures of wrapping material measuring up to 8 cm are visible on the face below the outer bandages, extending from the frontal bone to the chin, and covering the supraorbital margins, eyes, nose and mouth (Fig. 11).

4. Discussion

This case study provided a unique opportunity to both compare the oldest and newest forms of radiographic technology and to add the demographic and paleopathologic parts of knowledge on this particular ancient Egyptian mummy.

Conventional X-ray imaging has highly limited soft tissue contrast due to the overlapping range of attenuation values of different structures, limiting tissue-specific differentiation [6]. In 1981, Huebener and Pahl described the advantage of CT relative to conventional X-ray imaging in the assessment of soft tissues and inner organs in mummies, and highlighted the value of CT density (HU) values for the identification of wrapping or embalming materials [22]. Since its early applications in the 1970s, the quality of CT imaging has improved extensively. Multiplanar reformatting (MPR) and 3D VRTs of multislice CT images are the current state-of-the-art CT tools for data evaluation in mummy research [23]. However, paleoradiological pitfalls still have to be considered, including postmortem alterations caused by mummification or/and embalming [23]. Identification of foreign objects can be facilitated via measurements of CT density, since attenuation values correlate with chemical composition [23,24].

Pectus excavatum (Fig. 9) is currently the most frequent deformity of the thoracic cage and has been known since ancient times [20]. The etiology of pectus deformities is unclear, but there is a correlation between the anomaly and certain inheritable connective tissue diseases [25]; none of which were identified in our case. In a separate study, researchers found a depressed anterior chest wall and a probable deformed costal arch suggesting pectus excavatum in an adult male inside the 5th dynasty mastaba of Niankhkhnum and Khnumhotep (c. 2400 BC) in Saqqara [26].

The authors postulate parasitic disease as a potential etiology of the child's hepatomegaly. Several parasites can cause hepatic enlargement, but moderate or marked hepatomegaly, particularly in Egypt, suggest schistosomiasis [27]. It must be noted that identification of specific parasites in ancient Egyptian medical texts is difficult [28], and there is no definitive mention of a specific organism that can be attributed to schistosomiasis in ancient Egyptian sources. However, there are prescriptions against haematuria described in papyrus Ebers and against intestinal bleeding in papyrus Chester Beatty VI, which could indicate supportive care of schistosomiasis symptoms [29].

The authors suspect that the lumbosacral transition anomaly combined with curvature of the thoracic and lumbar spine might have caused the subchondral lesion near the right sacroiliac joint due to accelerated degeneration from asymmetric load-bearing.

The occurrence of Harris lines in the leg bones of the child is an indicator of physiological stress. There are many conditions that can cause Harris lines, including starvation, septicemia, pneumonia, several infectious diseases, emotional stress, birth trauma, poor maternal health and weaning [30]; the cause in the actual case is indeterminate.

The longitudinally oriented gaps in the cortices of both femora (Fig. 10) are inconsistent with fracture patterns frequently observed in clinical situations. Although longitudinal fractures of

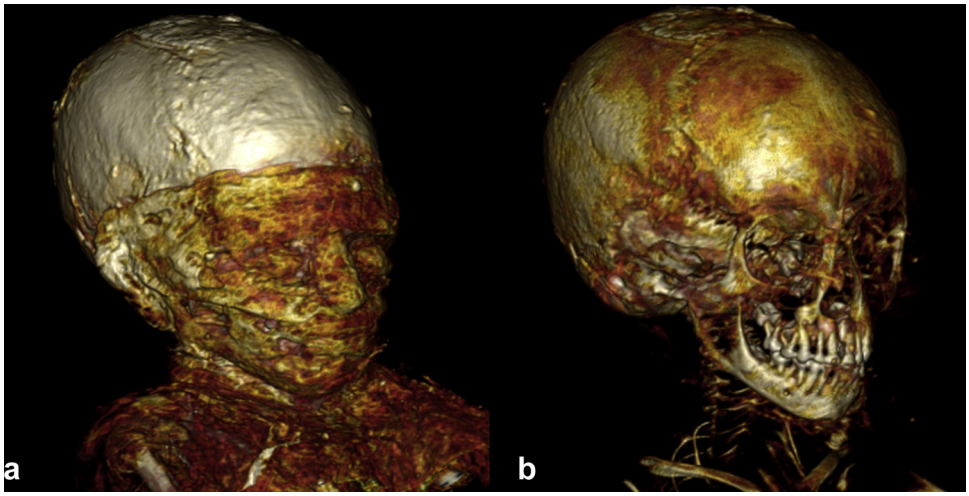

Fig. 11. 3D volume rendering illustrating hyperdense structures below the outer bandages, directly on the mummy's face extending from the supraorbital margins to the chin (a), and the facial skeleton below (b).

the medial cortex of the upper femoral shaft have been identified as a rare type of stress fracture predominantly seen in elderly and female patients [31], the cortical femoral shaft gaps in this specific case lack a physiological or biomechanical etiology. This suggests that the fractures have occurred post-mortem, possibly during the mummification procedure. As far as the authors know these findings are however novel within the mummification literature, and the exact source remains indeterminate.

Neither excerebration nor evisceration was observed. Desiccation of infant corpses without removal of brain or inner organs regularly occurred in ancient Egypt. There is no clear pattern relative to era and age at death for the treatment of the head of child mummies; however, one- to four-year-old child mummies generally show a higher rate of non-evisceration [10]. The preservation of the dehydrated brain and inner organs in this case is therefore coherent with prior observations.

The soft tissue shrinkage, especially on the extremities, indicates consistent desiccation by natural evaporation subsequent to the wrapping of the mummy by the embalmers. These observations are similar to the ones described by Panzer et al. [32].

The foreign substances inside the external auricular canals likely represent embalming materials (for example beeswax and coniferous resin), which were applied extensively to corpses, especially in later periods, due to their aromatic qualities and antibacterial properties [33]. The observed HU value (measuring up to 2079 HU) of the foreign substances in this specific case are however much higher than expected for resin (71HU [34]) or beeswax (-140 HU [22]). Thus, mineral components are likely, as described by Gostner et al. [24].

The hyperdense structures of wrapping material directly on the mummy's face (Fig. 11) possibly indicates a kind of mask modelled by the embalmers between the face and the outer bandages.

In conclusion, this case of ancient Egyptian child mummy highlights the remarkable progress made between the earliest X-ray technology and modern high-resolution CT; this demonstrates the immense potential of CT in mummy research, particularly in the identification of bony structures, soft tissues, body cavities, age at death, sex, paleopathological findings, artifacts, as well as mummification, embalming and wrapping techniques.

Applying high-definition CT enables standardized documentation and assessment of the above features, which subsequently can be used for quantitative comparison between different human mummies.

Acknowledgements

The authors thank Prof. Dr. Friedemann Schrenk (Senckenberg Research Institute, Frankfurt am Main) and Dr. Bernd Herkner (Senckenberg Museum of Natural History, Frankfurt am Main) for facilitating the re-examination of the mummy by dual-energy CT and approving soft tissue sampling for radiocarbon analysis. The authors also thank Dr. Ronny Friedrich, Susanne Lindauer, MSc. and Robin van Gyseghem, CTA for the technical support, for preparing and measuring the radiocarbon sample in the laboratory of Klaus-Tschira Archaeometry Centre at Curt-Engelhorn-Centre Archaeometry gGmbH Mannheim. In addition, many thanks to Dr. Uwe Busch (German Röntgen Museum, Remscheid-Lennep, Germany) for giving the permission to reproduce the historical X-ray image made by Walter Koenig in 1896.

References

[1] W. König, 14 Photographien mit Röntgen-Strahlen aufgenommen im Physikalischen Verein zu Frankfurt a. M., Johann Ambrosius Barth, Leipzig, 1896.
[2] P. Cosmacini, P. Piacentini, Notes on the history of the radiological study of Egyptian mummies: from X-rays to new imaging techniques, Radiol. Med. 113 (2008) 615–626.
[3] M.G. Fiori, M.G. Nunzi, The earliest documented applications of X-rays to examination of mummified remains and archaeological materials, J. R. Soc. Med. 88 (1995) 67–69.
[4] T. Böni, F.J. Rühli, R.K. Chhem, History of paleoradiology: early published literature, 1896–1921, Can. Assoc. Radiol. J. 55 (2004) 203–210.
[5] G.J. Conlogue, R.G. Beckett, Conventional radiography, in: R.G. Beckett, G.J. Conlogue (Eds.), Paleoimaging: Field Applications for Cultural Remains and Artifacts, CRS Press, Boca Raton, 2010, pp. 19–121.
[6] N. Lynnerup, F. Rühli, Short review: the use of conventional X-rays in mummy studies, Anat. Rec. 298 (2015) 1085–1987.
[7] R.K. Chhem, Paleoradiology: history and new developments, in: R.K. Chhem, D.R. Brothwell (Eds.), Paleoradiology: Imaging Mummies and Fossils, Springer, Berlin, Heidelberg, 2008, pp. 1–14.
[8] G. Saab, R.K. Chhem, R.N. Bohay, Paleoradiologic techniques, in: R.K. Chhem, D.R. Brothwell (Eds.), Paleoradiology: Imaging Mummies and Fossils, Springer, Berlin, Heidelberg, 2008, pp. 15–54.
[9] A.J. Nelson, R.K. Chhem, I.A. Cunningham, S.N. Friedman, G. Garvin, G. Gibson, et al., The ROM/UWO Mummy Project: a microcosm of progress in mummy research, in: H. Gill-Frerking, W. Rosendahl, A. Zink, D. Piombino-Mascali (Eds.), Yearbook of Mummy Studies, vol. 1, Verlag Dr. Friedrich Pfeil, München, 2011, pp. 127–132.
[10] R. Loynes, Prepared for Eternity. A Study of Human Embalming Techniques in Ancient Egypt Using Computerized Tomography Scans of Mummies Archaeopress Egyptology, 9, Archaeopress, Oxford, 2015.
[11] W. Rosendahl, D. Döppes, The radiocarbon method—basic principles and applications, in: B. Madea (Ed.), The Estimation of the Time Since Death, third ed., Taylor & Francis Ltd., New York, 2015, pp. 259–265.

[12] S. Panzer, M.R. Mc Coy, W. Hitzl, D. Piombino-Mascali, R. Jankauskas, A. Zink, et al., Checklist and scoring system for the assessment of soft tissue preservation in CT examinations of human remains, PLoS One 10 (8) (2015) e0133364.
[13] D.H. Ubelaker, Human Skeletal Remains: Excavation, Analysis, Interpretation, second ed., Taraxacum, Washington, DC, 1989.
[14] L. Scheuer, S. Black, Developmental Juvenile Osteology, Academic Press, London, 2000.
[15] M. Stloukal, H. Hanáková, Die Länge der Längsknochen altslawischer Bevölkerungen—Unter besonderer Berücksichtigung von Wachstumsfragen, Homo 29 (1978) 53–69.
[16] H. Schutkowski, Sex determination of infant and juvenile skeletons: I. Morphognostic features, Am. J. Phys. Anthropol. 90 (1993) 199–205.
[17] The Oxford History of Ancient Egypt, in: I. Shaw (Ed.), Oxford University Press, Oxford, 2000.
[18] T.D. White, P.A. Folkens, The Human Bone Manual, Elsevier Academic Press, Amsterdam, Boston, Heidelberg, 2005.
[19] B. Herrmann, G. Grupe, S. Hummel, H. Piepenbrink, H. Schutkowski, Prähistorische Anthropologie. Leitfaden der Feld- und Labormethoden, Springer, Berlin, Heidelberg, New York, 1990.
[20] A.C. Koumbourlis, Pectus deformities and their impact on pulmonary physiology, Paediatr. Respir. Rev. 16 (2015) 18–24.
[21] Ö.L. Konuş, A. Özdemir, A. Akkaya, G. Erbas, H. Celik, S. Isik, Normal liver, spleen, and kidney dimensions in neonates, infants, and children: evaluation with sonography, Am. J. Roentgenol. 171 (1998) 1693–1698.
[22] K.H. Hübener, W.M. Pahl, Computertomographische Untersuchungen an altägyptischen Mumien, Fortschr. Röntgenstr. 135 (1981) 213–219.
[23] F.J. Rühli, R.K. Chhem, T. Böni, Diagnostic paleoradiology of mummified tissue: interpretation and pitfalls, Can. Assoc. Radiol. J. 55 (2004) 218–227.
[24] P. Gostner, M. Bonelli, P. Pernter, A. Graefen, A. Zink, New radiological approach for analysis and identification of foreign objects in ancient and historic mummies, J. Archaeol. Sci. 40 (2013) 1003–1011.
[25] F. Tocchioni, M. Ghionzoli, A. Messineo, P. Romagnoli, Pectus excavatum and heritable disorders of the connective tissue, Pediatr. Rep. 5 (2013) 58–63.
[26] A.J. Bialas, J. Kaczmarski, J. Kozak, B. Kempinska-Miroslawska, Pectus excavatum in relief from ancient Egypt (dating back to circa 2400 BC), Interact. Cardiovasc. Thorac. Surg. 20 (2015) 556–557.
[27] M.M. Hassan, A.M. Farghaly, N.S. Gaber, H.F. Nageeb, M.H. Hegab, N. Galal, Parasitic causes of hepatomegaly in children, J. Egypt. Soc. Parasitol. 26 (1996) 177–189.
[28] J.F. Nunn, Ancient Egyptian Medicine, University of Oklahoma Press, Norman, 2002.
[29] J. Stephan, Die altägyptische Medizin und ihre Spuren in der abendländischen Medizingeschichte, Ägyptologie, vol. 1, Lit Verlag, Berlin, 2011.
[30] M.E. Lewis, The Bioarchaeology of Children. Perspectives from Biological and Forensic Anthropology, Cambridge University Press, Cambridge, 2007.
[31] M. Williams, J.D. Laredo, S. Setbon, G. Bélangé, M.A. Timsit, A. Karneff, et al., Unusual longitudinal stress fractures of the femoral diaphysis: report of five cases, Skelet. Radiol. 28 (1999) 81–85.
[32] S. Panzer, F. Borumandi, J. Wanek, C. Papageorgopoulou, N. Shved, G. Colacicco, et al., Modeling ancient Egyptian embalming: radiological assessment of experimentally mummified human tissue by CT and MRI, Skelet. Radiol. 42 (2013) 1527–1535.
[33] J.H. Taylor, Death and the Afterlife in Ancient Egypt, University of Chicago Press, Chicago, 2001.
[34] G. Sigmund, M. Minas, The Trier mummy Pa-es-tjau-em-aui-nu: radiological and histological findings, Eur. Radiol. 12 (2002) 1854–1862.